

Seismic Tomography and Monitoring of Magmatic Geothermal and Natural Hydrothermal Systems in the South of Bandung, Indonesia

P. Jousset¹, R. Sule², W. Dinningrat³, D. Syahbana⁴, A. Gassner¹, F. Akbar², S. Guichard¹, N. Schuck¹, R. Ryannugroho², A. Hendryana^{1,2}, Y. Kusnadi³, A. Nugraha², U. Muksin¹, M. Jaya⁵, B. Pratomo³, K. Erbas¹, D. Bruhn¹.

¹ Helmholtz Centre Potsdam GFZ German Research Centre for Geosciences, Telegrafenberg, 14473 Potsdam, Germany.

² Institut Teknologi Bandung, Faculty of Mining and Petroleum Engineering, Bandung, Indonesia

³ Star Energy Limited, Jakarta, Indonesia

⁴ Center of Volcanology and Geological Hazard Mitigation, Bandung, Indonesia

⁵ SGS Horizon B.V., The Netherlands; Formerly: Helmholtz Centre Potsdam GFZ

contact: p.jousset@gfz-potsdam.de

Keywords: Imaging, seismic tomography, fluid, volcanism, tectonic, earthquakes.

ABSTRACT

We assess geothermal resources from our understanding of the structure and the dynamics of geothermal reservoirs and hydrothermal systems in the south of Bandung. The co-existence of a large variety of intense surface manifestations like geysers, hot-steaming grounds, hot water pools, and active volcanoes suggest an intimate coupling between volcanic, tectonic and hydrothermal processes in this area. We deployed a geophysical network starting with a network of 30 seismic stations including high-dynamic broadband Güralp and Trillium sensors (0.008 - 100 Hz) and 4 short-period (1 Hz) sensors from October 2012 to December 2013. We extended the network in June 2013 with 16 short-period seismometers. Finally, we deployed a geodetic network including a continuously recording gravity meter, a GPS station and tilt-meters. In this paper we describe the set-up of the seismic and geodetic networks and we discuss first observations and results. The earthquakes locations were first estimated using a non-linear algorithm, and revealed at least 3 seismic clusters. We perform joint inversion of hypocenters and VP velocity 1D and 3D tomography. We discuss the resulting seismic Vp structure and the seismic activity pattern within the area and relate the structure to the distribution of hydrothermal systems. We aim at searching possible structural and dynamical links between different hydrothermal systems. In addition, we discuss possible dynamical implications of those volcanic systems from temporal variations of inferred parameters. The integration of those results allows us to achieve a better understanding of the structures and the dynamics of those geothermal reservoirs. This approach contributes to the sustainable and optimal exploitation of the geothermal resource in Indonesia.

1. INTRODUCTION

Soaring world population and emergence of nations from developing to industrial countries result in an increasing energy requirement and increase in prices of conventional energy resources. In this context, geothermal energy utilization rises, as it provides cleaner, cheaper and safer renewable source of energy. The exploration of new geothermal reservoirs and the monitoring of exploited geothermal reservoirs are both required to ensure human activities for sufficient energy supply and sustainable management of the geothermal resources. Geothermal resources are located in the Earth crust where increased heat flux and sufficient permeability to host fluids at depth is found (Huenges, 2010). Increased heat flow occurs in places like continental margins with subduction induced melting of the subducting plate, graben-structures, middle oceanic ridges and other spots where heat reaches crustal levels due to mantle convection and heats up shallow crustal layers.

The exploration of geothermal reservoirs can be performed with a number of techniques including geochemical and geological prospecting, and geophysical exploration methods, including resistivity (Arnason et al., 2010), active seismics (e.g., Krawczyk et al., 2015). Passive (broadband) seismology is a cost-effective way to image underground structures (e.g. reservoir structures, faults etc.) and movements by analyzing earthquake data (e.g., Jousset et al., 2010; Jousset et al., 2011), especially in geological settings where seismicity is significantly high, like Indonesia.

This study takes part of the framework of the Indonesian-German cooperation in geothermal studies (Erbaş et al., 2014). Seismological methods are powerful tools to be applied for geothermal exploration when geothermal sites are located in areas of intense local seismic activity (Jousset et al., 2011; Muksin et al. 2013A; 2013b). In the south of Bandung, several geothermal systems are present, together with intense superficial seismic activity (and active volcanoes, e.g., Syahbana et al., 2014). For example, the Wayang Windu geothermal system is a bi-phasic reservoir located in the center of this large volcanic complex and associated with Wayang, Windu and Bedil volcanoes (Figure 1).

2. SEISMIC NETWORKS AND DATA ANALYSIS

2.1 Network and stations

The deployment of a passive seismic network around geothermal areas in the South of Bandung was performed in several steps. It aims at detecting local and regional earthquakes and uses them as probe of the structure and stress changes in the volcanic complex.

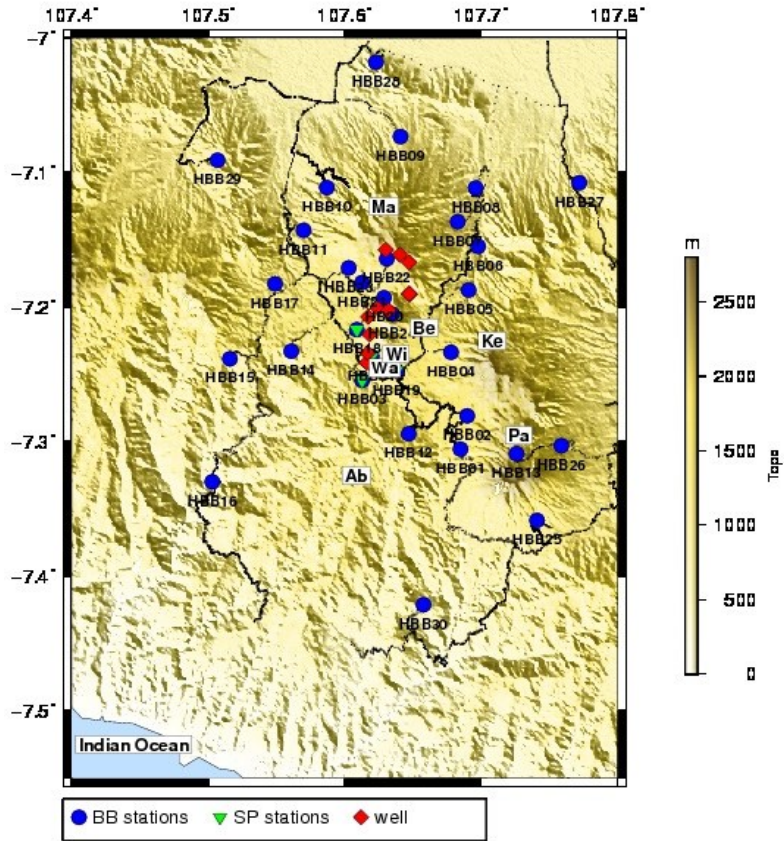


Figure 1: Seismic network deployed in the south of Bandung (2012-2013). Bandung is few km north of station HBB28. Blue circles are locations of the seismic stations; red dots are locations of the geothermal wells; Green triangles are locations of 4 short period stations. The additional 18 short-period stations deployed in June 2013 are not shown. Square symbols with 2 letters represent volcanoes location: Ab: Abig; Be: Bedil; Ke: Kendang; Ma: Malabar; Pa: Papandayan; Wa: Wayang; Wi: Windu;

Forty-eight seismometers were deployed from October 2012 until December 2013. We started with a network of 30 seismic stations (Fig 1.) including high-dynamic broadband Güralp (Fig. 2) and Trillium sensors (0.008 - 100 Hz) and 4 short-period (1 Hz) sensors. Four additional broadband sensors and 16 short-period sensors were added in June 2013. Data loggers are Earth Data Loggers (Fig. 3) or Cube (Omnirecs).



Figure 2: (left) Detail of the set-up of a broad band Güralp seismometer. (right) Station set-up example. The solar panel is fixed on the top of the container where the seismometer is deployed. The box outside contains the EDL data logger (Geophysical Instrument Pool of Potsdam equipment).

2.2 Seismic data analysis

Following the approach described in Jousset et al. (2010; 2011), we analysed the seismic records using a semi-automated processes. In order to select seismic events for travel time tomography, we first detected events at each station with a classical STA/LTA algorithm (Fig. 3). On the basis of the number of detections for a single event at each station, a first classification of the earthquakes is automatically performed. For each earthquake, the identification of P- and S-waves is then manually performed in order to “pick” arrival times at each station. A quality check of the picks is ensured using a double-pick technique instead of classical single pick and the reference to an Akaike Information Criteria (Akaike, 1978). In addition, the Wadati diagram is used to identify outliers in the picking and estimate roughly the VP/VS ratio.

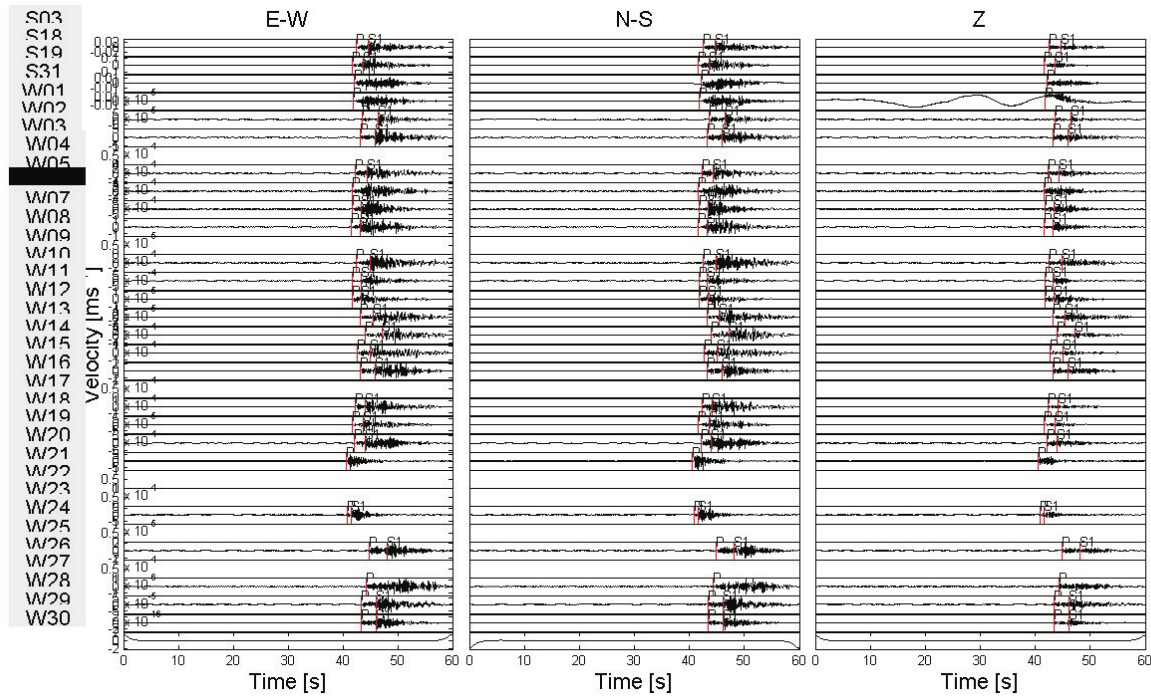


Figure 3: Seismograph 3-component records of a local micro-earthquake detected by at least 23 seismic stations. Vertical lines indicate arrival times for P and S waves manually picked with a Matlab interface tool Seismotool (Jousset et al., 2011).

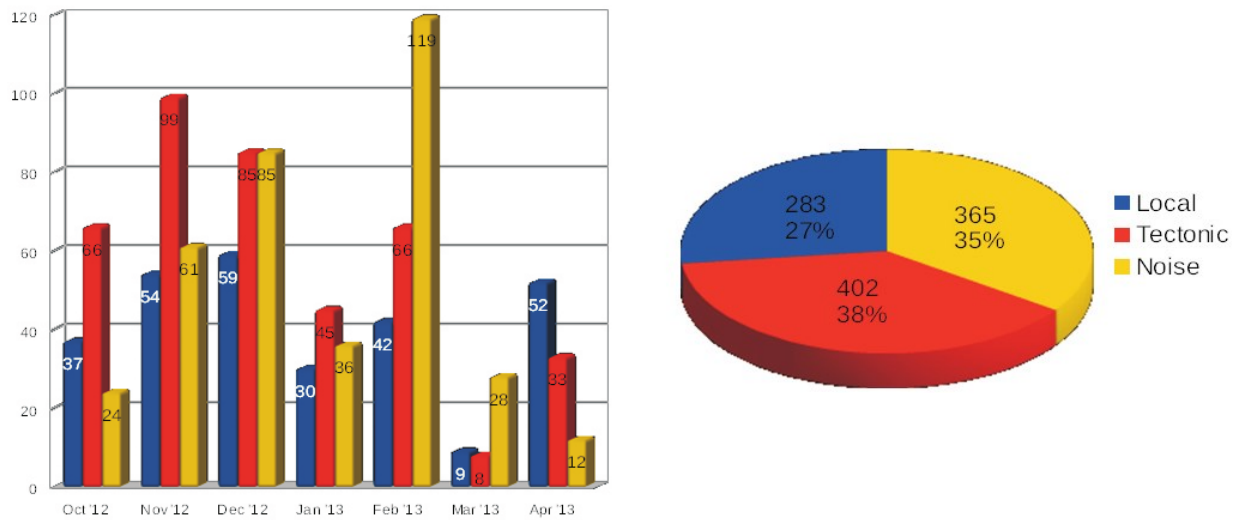


Figure 4: Statistics of detected and classified events (left) histogram representation with time (right) Percentage of each of the detected events for the considered period. Note that teleseismic events are included in the tectonic class.

A threshold time difference between S and P-wave arrival time of less than three seconds allows us to classify the first order earthquake type and location: we define local micro-earthquakes, regional tectonic earthquakes or teleseismic earthquakes (Fig. 4). Between October 2012 and April 2013, we have determined more than 350 local earthquakes events in the Wayang Windu area using the non-linear algorithm.

We then performed a preliminary location using a non-linear localization algorithm, which automatically determines earthquake or micro-earthquake hypocenters in these regions. The non-linear algorithm for locating local earthquakes is the following (Jousset et al., 2013): we assume a constant velocity model. The space below the network is parametrized as a 3D grid of nodes, where the velocities V_P and V_S and density are assumed. We compute the travel time of waves from each node of the parametrization modelled grid to all stations locations of the network. Then we compare in the least square sense the computed travel times with the observed travel times. The picking uncertainty is used as the error for the minimization. The result is the probability density function of being at the misfit minimum, chosen as the earthquake location (Fig. 5).

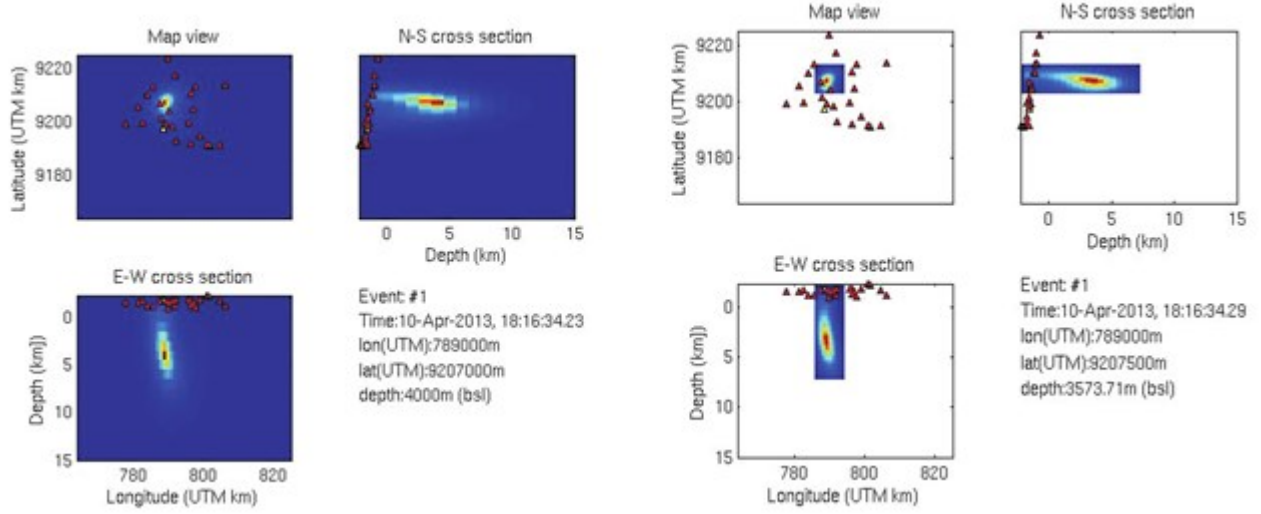


Figure 5: Non-linear localisation algorithm. The probability density function of being at the minimum of the misfit function between computed and observed travel times is shown with colour scale. Warm colours indicate high probabilities and blue represent low probability. (left) Result after the first iteration, showing the pdf in the whole grid with coarse resolution. (right) Result after the second iteration, showing the pdf in a section of the grid with finer resolution. The hypocenter location is taken at the highest probability of the pdf.

3. SEISMIC VP TOMOGRAPHY FOR INTEGRATED GEOPHYSICAL STRUCTURE OF THE RESERVOIRS

3.1 1D VP inversion and depth of the perturbations

A large number of authors (e.g., Thurber, 1983; 1986; 1993; Kissling, 1988; Ellsworth et al., 1991; Eberhart-Phillips, 1993; Iyer and Hirahara, 1993; Kissling et al., 1994; Tryggvason et al., 2002; Koulakov et al., 2007; Muksin et al., 2013a) have described details of the theory of local tomography inversion method. Two steps are required: 1. joint inversion for the 1-D velocity model and hypocentre locations, followed by 2. joint inversion for the 3-D velocity model and hypocentre locations.

The first step involves determining jointly the earthquake locations and the 1-D velocity model used in the hypocenter computation, using arrival time data for the 354 detected earthquakes; station corrections are used to adjust residual errors and are most likely due to surface effects. Following Husen et al. (1999), for each set of the performed inversions we used a wide range of starting velocity models to estimate the resolution of the 1-D inverted model, assuming a constant average. We used apriori earthquakes locations determined using the non-linear algorithm. We performed travel time tomography inversion, using several initial conditions for the number and the thickness of layers, surface velocity and velocity gradient. For each of several cases of number and thickness of layers, we performed 225 inversions with 25 various initial velocities at the surface and 25 values of the velocity vertical gradient.

Table 1: Example of depth for layers of initial 1D velocity models. For each of those layer repartition, 25 initial values of the velocity (1.2 km.s^{-1} until 2.9 km.s^{-1}) at surface layer were tested. For each of the initial velocity, 25 values of the vertical gradient of the velocity were tested. Results for each of those 3 examples are shown in Figure 6. Note that we tested more cases (Guichard, 2014), which are not represented here. Final inversion are similar for all the models.

Initial model	Layer 1	Layer 2	Layer 3	Layer 4	Layer 5	Layer 6	Layer 7	Layer 8	Layer 9
(a)	-2.5	1.0	2.0	4.0	6.0	10.0	13.0	-	-
(b)	-2.5	-1.5	1.0	1.5	2.0	3.0	4.0	13.0	-
(c)	-2.5	0.0	1.0	2.0	3.0	3.5	4.0	6.0	13.0

The results reveal that final shallow VP velocities and deep velocity do not show large dispersion, whereas the intermediary velocities (between -1 and -4 km depths) are more scattered. This result may point to 3D velocity variations due to the presence of geothermal reservoirs.

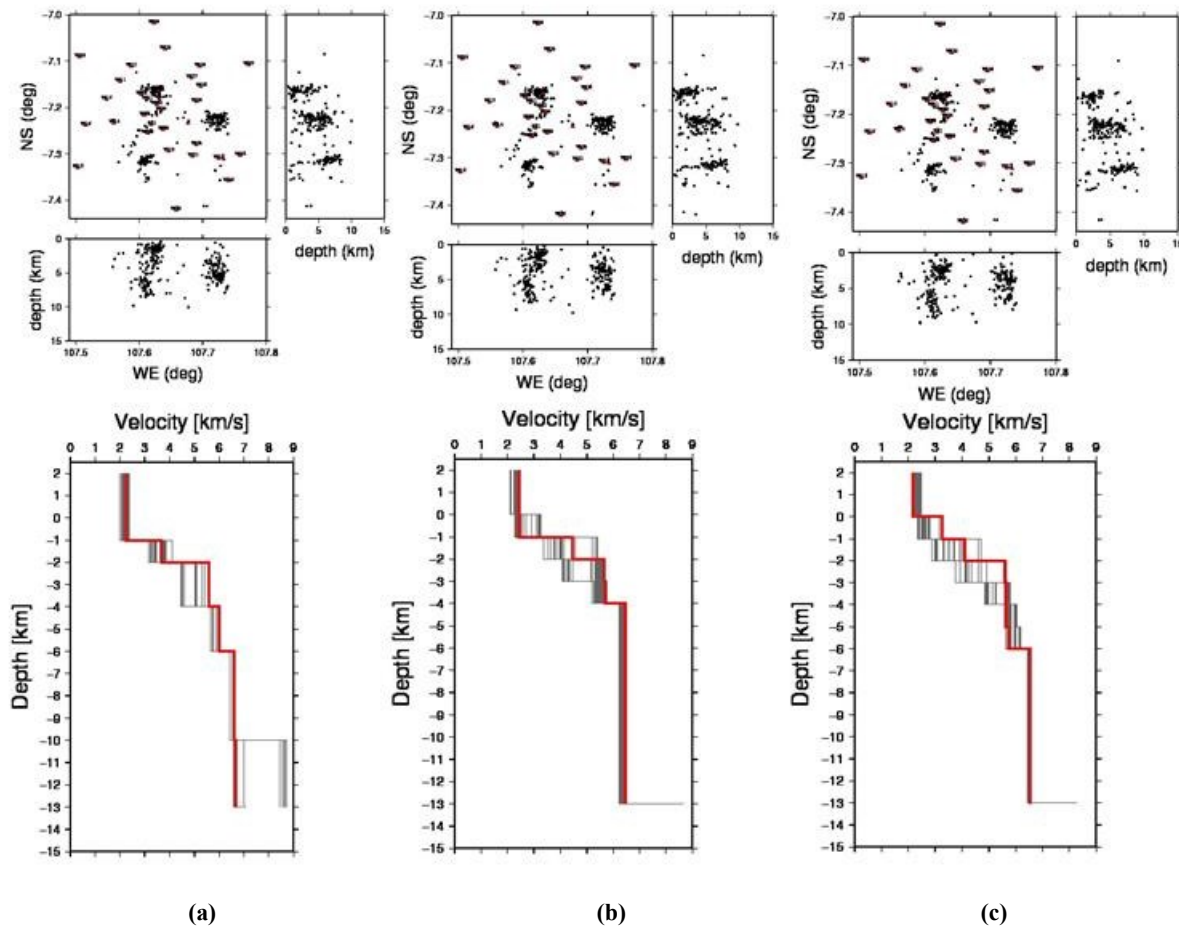


Figure 6: Earthquake locations and final 1D velocity models for several initial velocity 1D model. Note that the final results are independent on the initial model, pointing to a robust result. (a),(b) and (c) are results obtained with 7, 8 and 9 layers, respectively (see table 1).

3.2 3D joint inversion

The second step of our tomography involves inversion of the P- wave velocity model using SIMULSP12 (Evans et al., 1994), with the 1-D model and earthquake locations, as *a priori* information. As suggested by Evans et al. (1994), we first filter out all earthquakes for which the azimuthal distribution of stations around the epicenter leaves an angular gap greater than 180 degrees. The number of earthquakes in the reduced data set drops down to 324 earthquakes. Several methods have been proposed to parametrize the structure. We parametrize the structure by the VP velocity values at the nodes of a 3-D grid, possibly irregular. The observed P- and S- arrival times are inverted to simultaneously determine the coordinates of earthquake hypocentres and the values of velocities at the grid nodes. The solution is obtained by iterative damped least squares inversion (Evans et al., 1994). For each iteration, new ray paths are determined and the hypocentre solution is computed. Weighting is applied to each observation based on the size of the travel time residual and source-receiver distance. A damping parameter is used to stabilize the inversion (Eberhart-Phillips, 1993). Due to the source- and station distribution, the model volume is irregularly sampled. Estimating model fidelity or resolution in earthquake tomography may be performed by several means, e.g., inspecting the diagonal elements of the resolution matrix (Roeker, 1982), or by evaluating reconstructed synthetic models (e.g., checkerboards) for the specific earthquakes/station geometry (Humphreys and Clayton, 1988; Eberhart-Phillips and Michael, 1998).

Figure 7 shows results for several depths. For each depth, we note a similar pattern. A high velocity anomaly is visible in the west part of Waynag, Windu and Bedil volcanoes. A low VP velocity anomaly is clearly identified with SE-NW trend and extending from Papandayan volcano until the NW side of the Wayang Windu complex. The low velocity anomaly indicates a structural relationship between Wayang Windu and Papandayan volcano. Note that the resolution is poor, indicating that more picks should be included in the inversion for improved results.

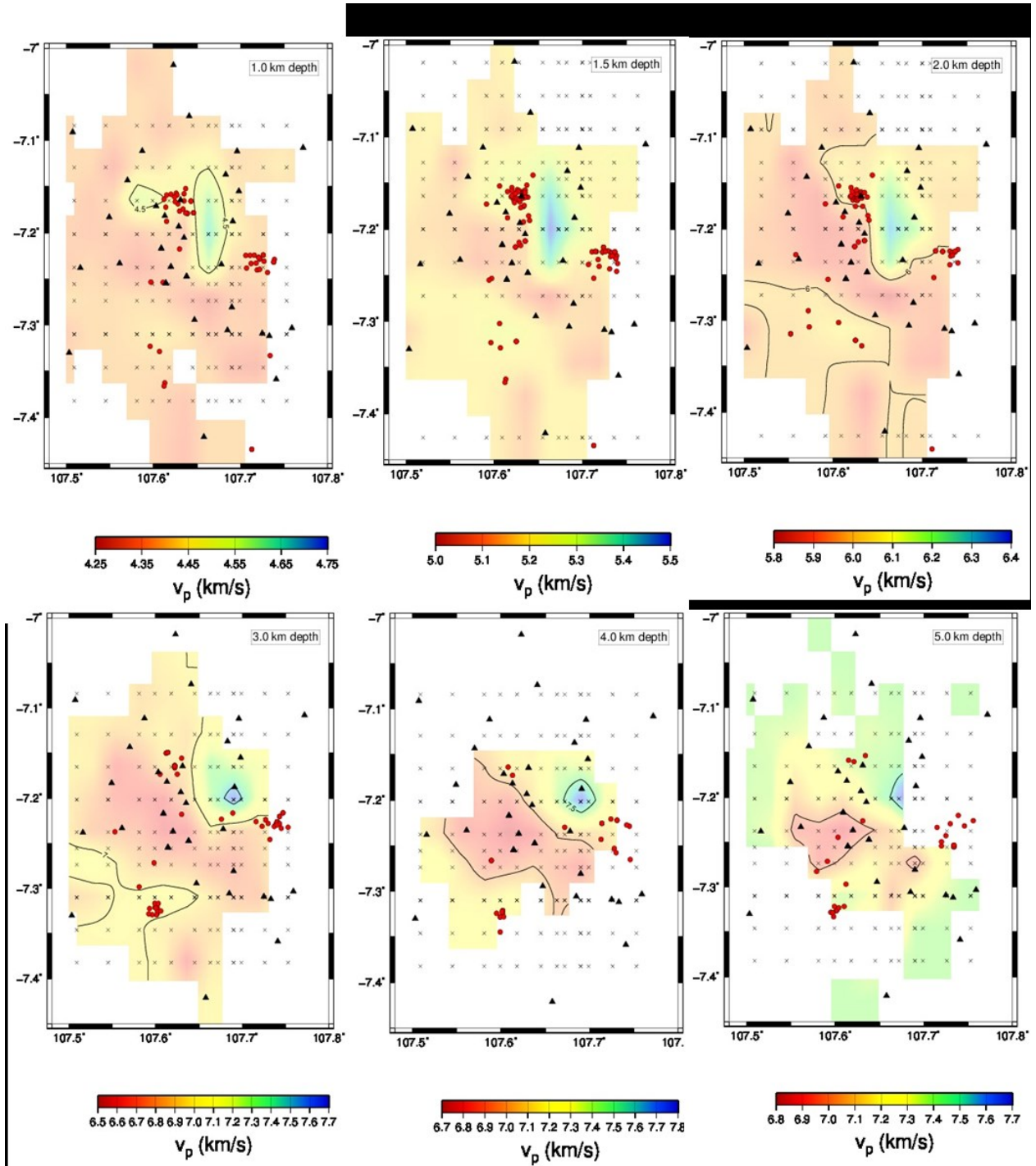


Figure 7: Horizontal slices of the V_p velocity model resulted from the joint inversion of P- and S-waves travel times from 324 local earthquakes. Each slice has its own color scale. Black triangles are the locations of the seismic stations. Red circles are the locations of the relocated earthquakes, taken between ± 500 m above and below the slice depth indicated in the upper right corner of each slice. A low velocity anomaly is highlighted by redish colors at each depth and has its root at 5 km depth, possibly deeper. This anomaly spread along a direction NW-SE and suggests a structural link between Papandayan volcano and the south of Wayang Windu volcanic complex. A high V_p velocity anomaly seems to correspond to the Wayang Windu Bedil volcanic complex and may be interpreted by high velocities due to the cooled magma.

5. CONCLUDING REMARKS AND PERSPECTIVES

Geophysical investigations of the geothermal province in the south of Bandung have been carried out both in terms of structure and dynamics.

In order to improve the knowledge of the structure, we performed a travel time tomography based on the analysis of detected earthquakes recorded by a network of more than 50 seismometers deployed in the south of Bandung.

The detection and the picking of arrival times of P- and S- waves allowed us the joint inversion of 1D and 3D velocity model and earthquake location. Results of the 1D velocity model are not dependent on the initial 1D model (velocity distribution, number of layers), pointing to a final robust solution for the 1D velocity model. 3D joint inversion results indicate a low velocity anomaly at all depths from 1 to 5 km in the NW – SE direction and establishing a structural link between Papandayan volcano and the West and South of Wayang and Windu volcanoes (see locations in Figure 1). A positive VP anomaly seems correlated with the Wayang-Windu-Bedil magmatic complex. In order to increase the resolution at the surface, we are currently performing ambient noise tomography, and we will compare both models.

Three seismic clusters are found in the area. Two of those clusters are associated with geothermal areas (Gunung Malabar and Gunung Kendang); one identified seismic cluster was unknown earlier (not detected) and is located at the southern border of the low velocity anomaly (Gunung Abig), possibly indicating the presence of fluids at depth in this area.

In order to monitor the dynamic feature of this vapor bi-phasic reservoir, we also deployed a geodetic network, including a continuously recording gravity meter, a GPS station, tiltmeters and a meteo station. We hope to track fluid movements in the structure found. We will also perform Earth Tide analysis, which will be very useful for removing accurate local tidal model and gravity surveys performed in the area.

ACKNOWLEDGEMENTS

The authors thank the Indonesian partners from Ministry for Science and Technology RISTEK, Agency for the Assessment and Application of Technology (BPPT), Star Energy Geothermal (Wayang Windu) Limited. The seismic stations are provided partly by the Geophysical Instrumental Pool of Postdam (GIPP). Arkadindo provided the station construction materials and constructed the stations. The German Federal Ministry for Education and Research is funding this German projects under grants 03G0753A&B and 03G0834A.

REFERENCES

- Akaike H., 1978. A Bayesian analysis of the minimum AIC procedure. *Annals of the Statistical Mathematics* 30, 9-14.
- Árnason, K., Eysteinnsson, H., Hersir, G., 2010. Joint 1D inversion of TEM and MT data and 3D inversion of MT data in the Hengill area, SW Iceland. *Geothermics* 39, 13–34.
- Erbas K., P. Jousset, M. S. Jaya, F. Deon, M. Nukman, M. Umar, S. W. Niasari, M. Andhika, M. Brehme, A. Keserovic, Wiyono, E. Huenges, 2014. German-Indonesian cooperation on sustainable geothermal energy – status and perspective. ITB Workshop, Bandung, 5-6 march 2014.
- Eberhart-Phillips, D., 1993. Local earthquake tomography: earthquake source region, pages 613–643. Eds Iyer, H.M and Hihara K. and Chapman & Hall, London.
- Eberhart-Phillips, D. and Michael, A. J., 1998. Seismotectonics of the Loma Prieta, California, region determined from three-dimensional , , and seismicity. *J. Geotherm. Res.* 103(B9):21099–21120.
- Ellsworth, W. L., Eberhart-Phillips, D., and Kissling, E., 1991. A test of local earthquake tomography. *Seism. Res. Lett.*, 62:31.
- Evans, J. R., Eberhart-Phillips, D., and Thurber, C. H., 1994. User's manual for SIMULPS12 for imaging and : a derivative of the "thurber" tomographic inversion SIMUL3 for local earthquakes and explosions. USGS - Open-file report, 94-431:1–101.
- Guichard S., 2014. Seismic tomography studies on geothermal fields and volcanoes in West Java, Indonesia. Bachelor thesis Helmholtz Center Potsdam GFZ – Leibniz Universität Hannover, 64 pp.
- Huenges, E., 2010. *Geothermal Energy Systems: Exploration, Development and Utilization*. Wiley-vch Verlag, GmGH & co, KgaA, ISBN-13: 978-3527408313.
- Humphreys, E. and Clayton, R. W., 1988. Adaptation of back projection tomography to seismic travel time problems. *J. Geophys. Res.*, 93:4731–4735.
- Husen, S., Kissling, E., Flueh, E., and Ash, G., 1999. Accurate hypocentre determination in the Seismogenic Zone of the subducting Nazca plate in the northern Chile using a combined on/off-shore network. *Geophys. J. Int.*, 138:687–701.
- Iyer, H. M. and Hirahara, K., 1993. *Seismic Tomography: Theory and practice*. Chapman and Hall, London, UK.
- Jousset, P., Haberland, C., Bauer, K., Arnason, K., Weber, M., and Fabriol, H., 2010. Seismic tomography and long-period earthquakes observation and modelling at the Hengill geothermal system. *Proceedings World Geothermal Congress, Bali*, 25-29 April 2010, 7 pages.
- Jousset P., C. Haberland, K. Bauer and K. Arnason, 2011. Hengill geothermal volcanic complex (Iceland) characterized by integrated geophysical observations. *Geothermics* 40, 1-24.
- Jousset P., A. Budi-Santoso, A. D. Jolly, M. Boichu, Surono, S. Dwiyo, S. Sumarti, S. Hidayati, P. Thierry, 2013. Signs of magma ascent in LP and VLP seismic events and link to degassing: An example from the 2010 explosive eruption at Merapi volcano, Indonesia, 261, 171-192.
- Kissling, E., 1988. Geotomography with local earthquake data. *Rev. Geophys.*, 26:659–698.
- Kissling, E., Ellsworth, W., Eberhart-Phillips, D., and Kradolfer, U., 1994. Initial reference models in local earthquake tomography. *J. Geophys. Res.*, 99:19635–19646.

- Koulakov, I., Bohm, M., Asch, G., Luehr, B.-G., Manzanares, A., Brotopuspito, K. S., Fauzi, P., Purbawinata, M. A., Puspito, N. T., Ratdomopurbo, A., Kopp, H., Rabbel, W., and Shevkunova, E. (2007). P and S velocity structure of the crust and the upper mantle beneath central Java from local tomography inversion. *J. Geophys. Res.*, 112(B08310).
- Krawczyk, C. M., U. Polom, W. Wiyono, B. Pramono, 2015. Tailoring reflection seismic experiments to geothermal exploration targets in Indonesia, WGC 2015.
- Muksin U., K. Bauer, C. Haberland, 2013a. Seismic Vp and Vp/Vs structure of the geothermal area around Tarutung (North Sumatra, Indonesia) derived from local earthquake tomography *Journal of Volcanology and Geothermal Research* 260, 27-42.
- Muksin, U., Haberland, C., Bauer, K., Weber, M., 2013b. Three-dimensional upper crustal structure of the geothermal system in Tarutung (North Sumatra, Indonesia) revealed by seismic attenuation tomography, *Geophysical Journal International*, 195, 2037-2049.
- Roeker, S.W., 1982. Velocity structure of the Pamir-Hindu Kush region: possible evidence of subducted crust. *Journal of Geophysical Research* 87, 945–959.
- Syabhana D. K., C. Caudron, P. Jousset, T. Lecocq, T. Camelbeeck, A. Bernard, Surono, 2014. Fluid dynamics inside a “wet” volcano inferred from the complex frequencies of long-period (LP) events: An example from Papandayan volcano, West Java, Indonesia, during the 2011 seismic unrest. *Journal of Volcanology and Geothermal Research* 280, 76-89.
- Thurber, C. H., 1983. Earthquake locations and three-dimensional crustal structure in the Coyote Lake area, central California. *J. Geophys. Res.*, 88(B10):8226–8236.
- Thurber, C. H., 1986. Analysis methods for kinematic data from local earthquakes. *Rev. Geophys.*, 24:793–805.
- Thurber, C. H., 1993. Local earthquake tomography: velocities and -theory, pages 563–583. Eds Iyer, H.M and Hihara K. and Chapman and Hall, London.
- Tryggvason, A., Rögnvaldsson, S. T., and Flovenz, O. G., 2002. Three-dimensional imaging of the P and S-wave velocity structure and earthquake locations beneath Southwest Iceland. *Geophys. J. Int.*, 151:848–866.